

Article

Multi-Scroll Attractor and Multi-Stable Dynamics of a Three-Dimensional Jerk System

Fudong Li ^{1,*} and Jingru Zeng ²

¹ School of Mechanical and Electrical Engineering, Beijing Information Science and Technology University, Beijing 100192, China

² Department of Electrical Engineering, Chengnan College, Changsha University of Science & Technology, Changsha 410015, China

* Correspondence: 20182238@bistu.edu.cn

Abstract: A multi-scroll attractor reflects the structural diversity of the dynamic system, and multi-stability behavior reflects its state diversity. Multi-scroll and multi-stability chaotic systems can produce complex random sequences, which have important application values in the field of data security. However, current works on multi-scroll–multi-steady behavior have been carried out separately, rather than simultaneously. This paper considers a three-dimensional Jerk system with a sinusoidal nonlinear term. The basic dynamic behaviors, such as the stability of equilibrium points, bifurcation of parameters and initial values, phase diagrams, and basins of attraction, were analyzed. It was found that the system has infinite equilibrium points. Moreover, the system not only generates complex dynamics, such as single-scroll, double-scroll, and multi-scroll but also realizes the self-reproduction of these dynamic characteristics by controlling the initial value of the system. Therefore, by expanding the equilibrium point, the effective controls of the system’s structural diversity and state diversity are realized at the same time, having important theoretical significance and application value.

Keywords: Jerk system; multi-scroll; multi-stability; equilibrium point; diversity



Citation: Li, F.; Zeng, J. Multi-Scroll Attractor and Multi-Stable Dynamics of a Three-Dimensional Jerk System. *Energies* **2023**, *16*, 2494. <https://doi.org/10.3390/en16052494>

Academic Editors: Denis N. Sidorov and Fang Liu

Received: 25 August 2022

Revised: 21 September 2022

Accepted: 24 September 2022

Published: 6 March 2023



Copyright: © 2023 by the authors. Licensee MDPI, Basel, Switzerland. This article is an open access article distributed under the terms and conditions of the Creative Commons Attribution (CC BY) license (<https://creativecommons.org/licenses/by/4.0/>).

1. Introduction

A multi-scroll chaotic system, compared to a single-scroll chaotic system and a double-scroll chaotic system, has a more complex dynamical structure and richer dynamical behavior, so it has important application prospects in the fields of data security protection and information encryption [1–5]. At the same time, research into the generation mechanism of a multi-scroll attractor is helpful to understand the chaotic system, further promoting the development of chaos theory [6–12]. Compared with a fractional-order multi-scroll chaotic system, integer-order multi-scroll chaotic systems have more mature theoretical bases and mathematical analysis methods, attracting the attention of scholars [13–17]. Suykens constructed a multi-scroll system based on the Chua circuit for the first time [18]. Subsequently, scholars constructed a variety of multi-scroll chaotic systems on the basis of Chen’s system [19], the RCL network [20], and the Sprott system [21]. One can expand the index-2 equilibrium point of the system by introducing the polynomial function, piecewise quadratic function, hysteresis function, step function, saw tooth wave function, etc., to construct a multi-scroll chaotic system [22–25]. In addition, some other methods can be used to construct multi-scroll attractors. For example, the authors of [26] constructed a class of multi-scroll hybrid systems by selecting an appropriate unstable linear system and translation transformation. The authors of [27] reported on the construction scheme of a class of grid multi-scroll chaotic systems by designing a switched linear system and heteroclinic ring. The authors of [28] reported on a construction method of a multi-scroll system based on robust chaos by modifying the amplitude control factor and position control factor. A

grid multi-scroll chaotic system was reported and analyzed in reference [29] through translation, image, rotation, and other transformations. In reference [30], the authors constructed a class of hyper-chaotic multi-scroll systems without an equilibrium point. The Jerk system has a simple mathematical structure and is often used to design multi-scroll attractors. For example, the authors of [31] presented a multi-scroll chaotic attractor based on the Jerk model by introducing the sawtooth wave function. In [32], the authors found that the Jerk circuit, consisting of the sine function, could produce multi-scroll attractors, and that the number of scrolls depends on the simulation time. Then, a linear controller in the form of the Heaviside function was employed to select the number of scroll attractors.

In recent years, multi-stability has become an important research direction in the field of nonlinear dynamics. The multi-stability of a dynamical system means that the system has multiple solutions or multiple attractors under fixed parameters and different initial conditions [33]. Generally, multi-stability exists in symmetric and asymmetric systems. Based on the symmetry of the state variable, there may be symmetric coexistence attractors in the symmetric system. The asymmetric system may have symmetric or asymmetric coexistence attractors [34,35]. The coexistence of multiple attractors means that the system can provide multiple stable operating modes. When disturbed by external noise or other environmental uncertainties, the multi-stable system can maintain normal operation by switching different operating states. Therefore, a multi-stable system has flexible and robust dynamical behavior. At the same time, multi-stability can be used in the field of information engineering for pseudorandom number generation and data security protection. Therefore, it is of great theoretical significance and practical engineering value to study 'multi-steady' in a nonlinear system and a multi-stable dynamical system working in the expected oscillation state [36–39]. An effective strategy to realize the state control of a multi-stable system is to obtain multiple equilibrium points by introducing a periodic function and then achieving the desired stable oscillation behavior by selecting the initial value near the equilibrium point surrounded by the corresponding oscillation orbit.

Based on the above analysis, an important approach to constructing a dynamical system with multi-scroll attractors is to establish multiple invariant sets by expanding the number of index-2 equilibrium points of the original system; we can also obtain the desired multi-steady oscillation behavior by selecting the initial value near the unstable equilibrium point surrounded by one invariant manifold. On the other hand, the multi-scroll attractor reflects the structural diversity of the dynamical system, and the oscillation behaviors of multiple coexisting attractors reflect the state diversity of the system. Obviously, the chaotic system with multi-scroll attractors and multi-steady state dynamics will show more complex dynamical characteristics. However, the present research on the multi-scroll attractor and multi-steady oscillation of the dynamical system was basically carried out independently, which does not well reflect the complex dynamical characteristics of the nonlinear system. Therefore, constructing a dynamical system with both a multi-scroll attractor and multi-steady oscillation behavior will have more important theoretical significance and application value. In this paper, a three-dimensional Jerk system with a periodic sinusoidal nonlinear function was considered. It was found that the system has an infinite number of equilibrium points, and can generate complex dynamics, such as single-scroll, double-scroll, and multi-scroll attractors. Moreover, one can also achieve the self-reproduction dynamics in the system by selecting the position of the initial value on the coordinate axis. The main contribution of this paper is that we studied the multi-scroll behavior of the Jerk system, as well as its multi-stability dynamics, by introducing sine-type nonlinearity. Thus, the effective controls of structural diversity and state diversity were realized at the same time by expanding the equilibrium point, which has important theoretical significance and application value.

2. Model of Jerk System

The three-dimensional Jerk system with a sinusoidal nonlinear function is described by

$$\begin{cases} \dot{x} = y \\ \dot{y} = az \\ \dot{z} = -y - bz + c \sin(dx) \end{cases} \tag{1}$$

where a, b, c, d are the system parameters; x, y, z are the state variables. Considering the condition $\dot{x} = 0, \dot{y} = 0, \dot{z} = 0$, we obtain the line equilibrium point $(k\pi/d, 0, 0), k = 0, \pm 1, \pm 2, \pm 3 \dots$. Therefore, the system will produce hidden dynamical behavior. The Jacobian matrix can be given by

$$J = \begin{pmatrix} 0 & 1 & 0 \\ 0 & 0 & a \\ cd \cos(dx) & -1 & -b \end{pmatrix} \tag{2}$$

The characteristic equation of (2) is expressed as $-\lambda^3 - b\lambda^2 - a\lambda + acd \cos(dx) = 0$ based on the solution of $|J - I\lambda| = 0$. Thus, we have $\cos(dx) = \cos(k\pi)$ for the line equilibrium point. It obtains that $\cos(dx) = 1$ when $k = 0, \pm 2, \pm 4 \dots$ and $\cos(dx) = -1$ when $k = \pm 1, \pm 3, \pm 5 \dots$. We select $a = 2, b = 0.6, c = 0.8, d = 2$ for the sake of analyzing. Therefore, it yields

(1) When $\cos(dx) = 1$, it obtains the characteristic equation $-\lambda^3 - b\lambda^2 - a\lambda + acd = 0$ and the three characteristic roots $-0.5 + 1.4663i, -0.5 - 1.4663i, 0.4$. This means that when $k = 0, \pm 2, \pm 4 \dots$, the equilibrium point $(k\pi/d, 0, 0)$ is an unstable saddle focal equilibrium point set with index-1.

(2) When $\cos(dx) = -1$, it obtains the characteristic equation $-\lambda^3 - b\lambda^2 - a\lambda - acd = 0$ and the three characteristic roots $-0.0535 + 1.3944i, -0.0535 - 1.3944i, -0.493$. This means that when $k = \pm 1, \pm 3, \pm 5 \dots$, the equilibrium point $(k\pi/d, 0, 0)$ is a stable equilibrium point set.

We selected the parameter $b = 0.6, c = 1, d = 2$ and the initial condition $(-2\pi, 0, 0)$, and took parameter a as the bifurcation parameter. Figure 1a displays the bifurcation diagram produced by the local maxima of the state variable x ; the sample number of the bifurcation parameter was 800. Figure 1b displays the evolution process of the corresponding Lyapunov exponent spectra calculated by the orthogonal method with the simulation time $T = 5000$. It can be seen that with the increase of parameter a , the system entered a chaotic state through period-doubling bifurcation; the evolution of the Lyapunov exponent spectrum is consistent with the bifurcation diagram.

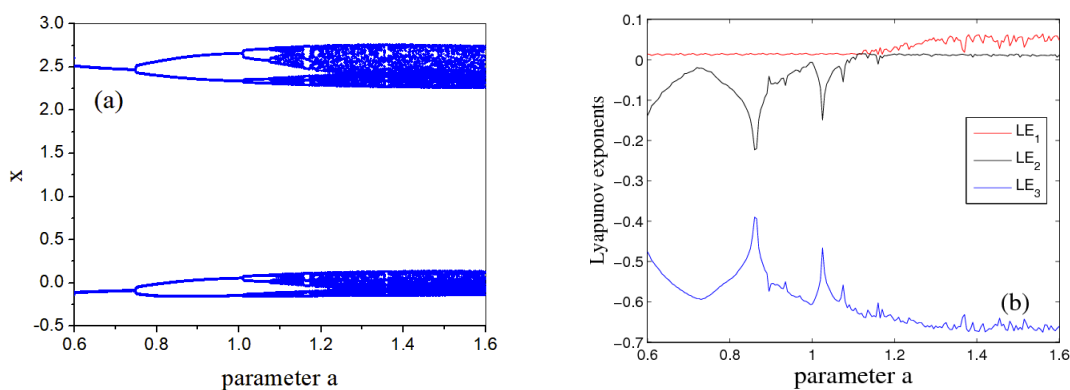


Figure 1. (a) Bifurcation diagram and (b) Lyapunov exponent spectra versus a .

3. Multi-Scroll Attractor of Jerk System

To explore the multi-scroll attractor in the reported Jerk system, the dynamics evolution versus parameter c was considered with the selection of parameters $a = 2, b = 0.6, d = 2$, and the initial condition $(0.1, 0.01, 0.1)$. As displayed in Figure 2, the dynamics

evolution is described by the bifurcation diagram of state variable x and the Lyapunov exponent spectra. It can be seen from Figure 2 that with the increase of parameter c , the system developed different movement patterns. Specifically, the system was in a stable period-1 state when $c \in [0.8, 0.926]$; the system was in the period-2 state when $c \in (0.926, 0.976]$; then it entered the chaotic state through the period-doubling bifurcation. The similar evolution process continued until $c = 1.697$. Then, the system entered the multi-branch chaotic state starting from $c = 1.697$, which indicated that the multi-scroll attractor behavior arose. Moreover, four obvious periodic windows were embedded in the multi-scroll chaotic region.

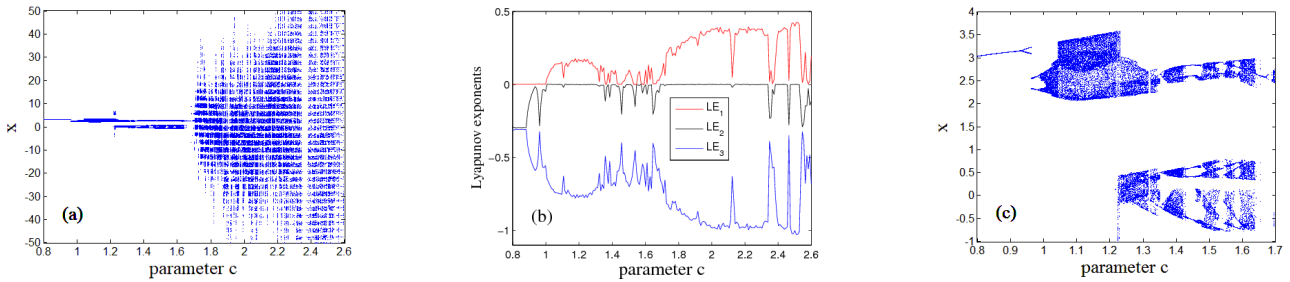


Figure 2. (a) Bifurcation diagram, (b) Lyapunov exponent spectra versus c , and (c) the enlarged drawing of (a).

In order to further confirm the evolution process of the system dynamics, some typical discrete values of parameter c were selected to draw the phase diagram of the system, as shown in Figure 3. When $c = 0.9$, the system showed the limit cycle state of the single scroll period-1; when $c = 0.95$, the system was in a single scroll period-2 state; when $c = 0.99$, the system was in a single scroll period-4 state; when $c = 1.1$, the system behaved as a single-scroll chaotic state; when $c = 1.25$, the system presented a double-scroll chaotic state; when $c = 1.44$, the system was in the state of a double-scroll period-2; when $c = 1.58$, the system was in the state of double-scroll period-4; and when $c = 1.8$, the system behaved as multi-scroll chaos behavior.

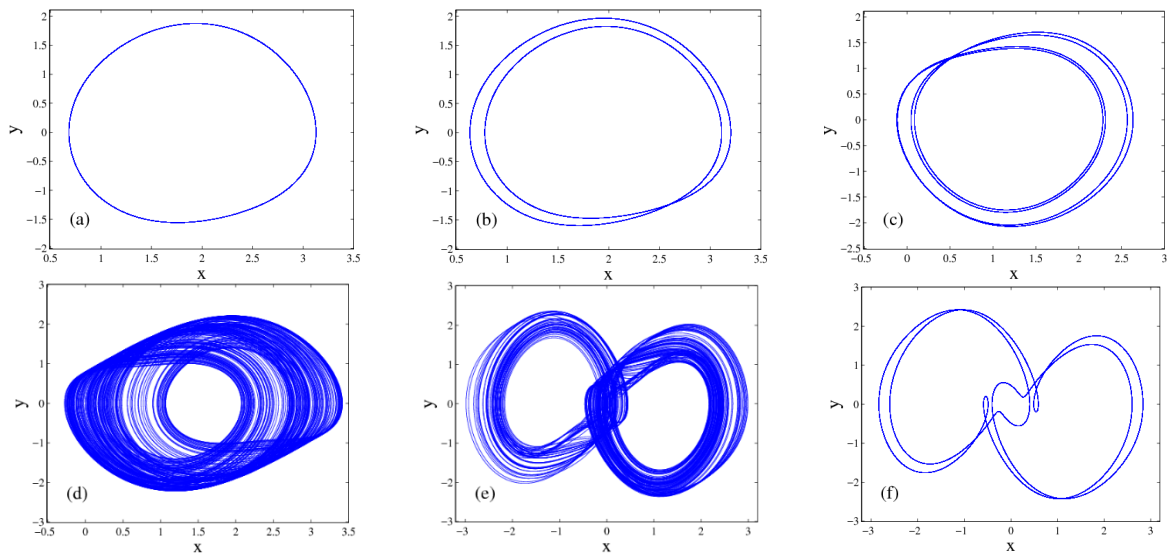


Figure 3. Cont.

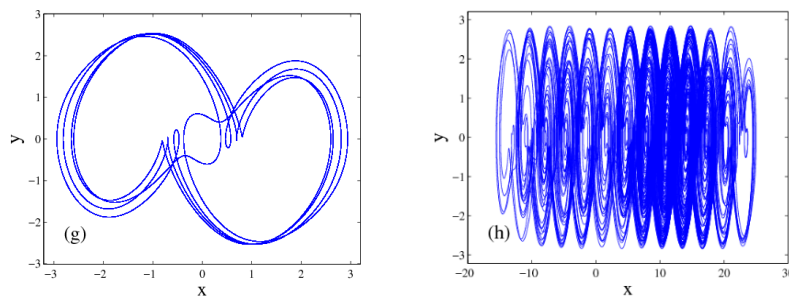


Figure 3. (a) Single scroll period-1 when $c = 0.9$; (b) single scroll period-2 when $c = 0.95$; (c) single scroll period-4 when $c = 0.99$; (d) single-scroll chaotic state when $c = 1.1$; (e) double-scroll chaotic state when $c = 1.25$; (f) double-scroll period-2 when $c = 1.44$; (g) double-scroll period-4 when $c = 1.58$; (h) multi-scroll chaos when $c = 1.8$.

We note that $\sin(dx)$ is a function with the period of $2\pi/d$, which means that when x moves to $x + 2k\pi/d$, $k \in \mathbb{Z}$, the right-hand side of the third equation of system (1) remains unchanged. Therefore, if the multi-scroll chaotic attractors exist, the distance of adjacent scrolls can be deduced as $2\pi/d$. This means that a larger k will bring a smaller distance between adjacent scrolls. The analysis can be numerically confirmed in Figure 4 with $d = \pi$ and $d = 2\pi$. It is known from Figure 4 that when parameter d is equal to π and 2π , the distances of the adjacent scrolls are, respectively, reckoned to 2 and 1, which is consistent with the theory analysis.

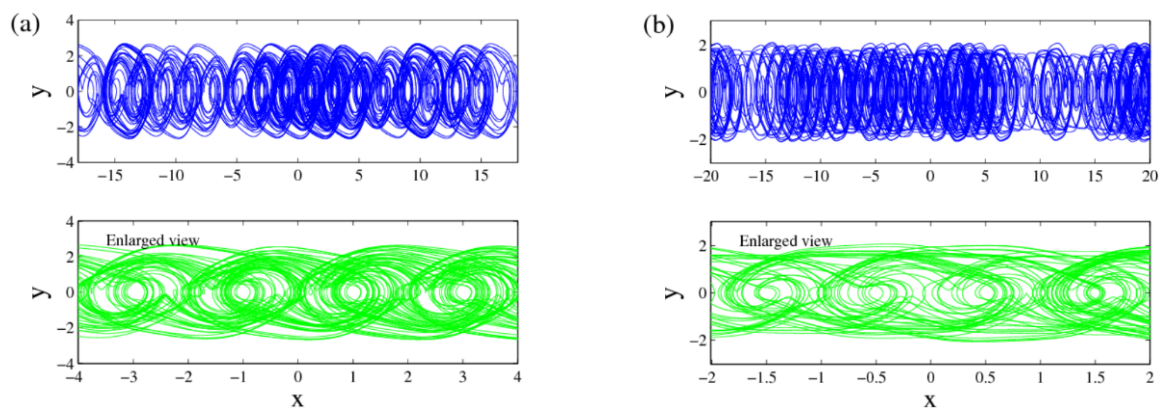


Figure 4. Multi-scroll chaotic attractors with (a) $d = \pi$ and (b) $d = 2\pi$.

4. Multi-Stable Dynamics of Jerk System

When selecting the parameter $a = 1.5$, $b = 0.6$, $c = 1$, $d = 2$, and initial condition $y_0 = 0.01$, $z_0 = 0.01$, the bifurcation diagram of state variable x and the evolution of the Lyapunov exponent spectra versus the initial condition x_0 are displayed in Figure 5. It can be seen that the initial value x_0 can realize the self-reproduction of the system dynamics along the x -axis and y -axis, and the reproduction period is π . Moreover, the periodic amplitude modulation of the system dynamics along the z -axis direction can be realized. Nevertheless, the dynamics complexity of the system remains unchanged, as shown by the constant Lyapunov exponent spectrum in Figure 5b.

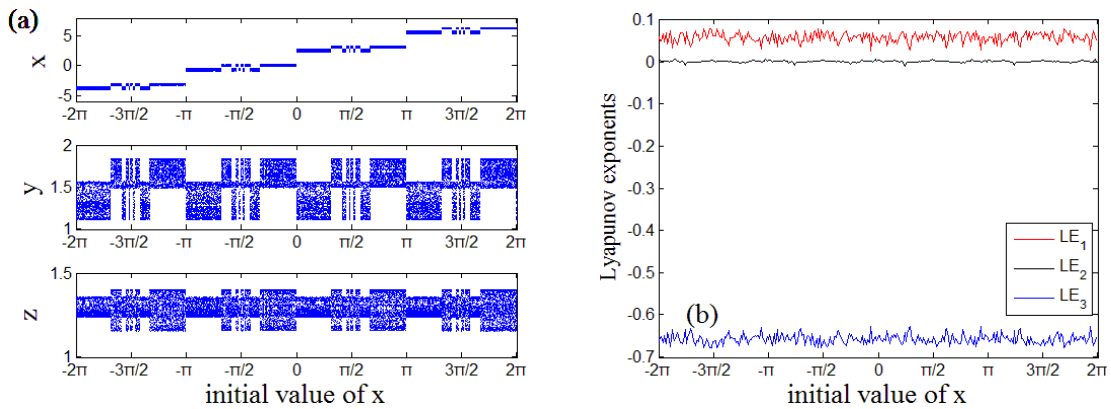


Figure 5. (a) Bifurcation diagram, (b) Lyapunov exponent spectra versus the initial value x_0 .

As mentioned above, under the selection of parameters $a = 2, b = 0.6, d = 2$, and initial condition $x_0 = 0.1, y_0 = 0.01, z_0 = 0.01$, the system showed complex motions, such as a single-scroll period-2 state, single-scroll chaotic state, double-scroll chaotic state, double-scroll period-4 state, and multi-scroll chaotic state. According to Figure 5, when the initial value x_0 of the system changed periodically, the self-reproduction of the system attractor could be realized. In the numerical experiment, the initial value x_0 was periodically selected at the interval π to obtain the self-reproduction behavior of different values of parameter c , as depicted by the phase diagrams in Figure 6.

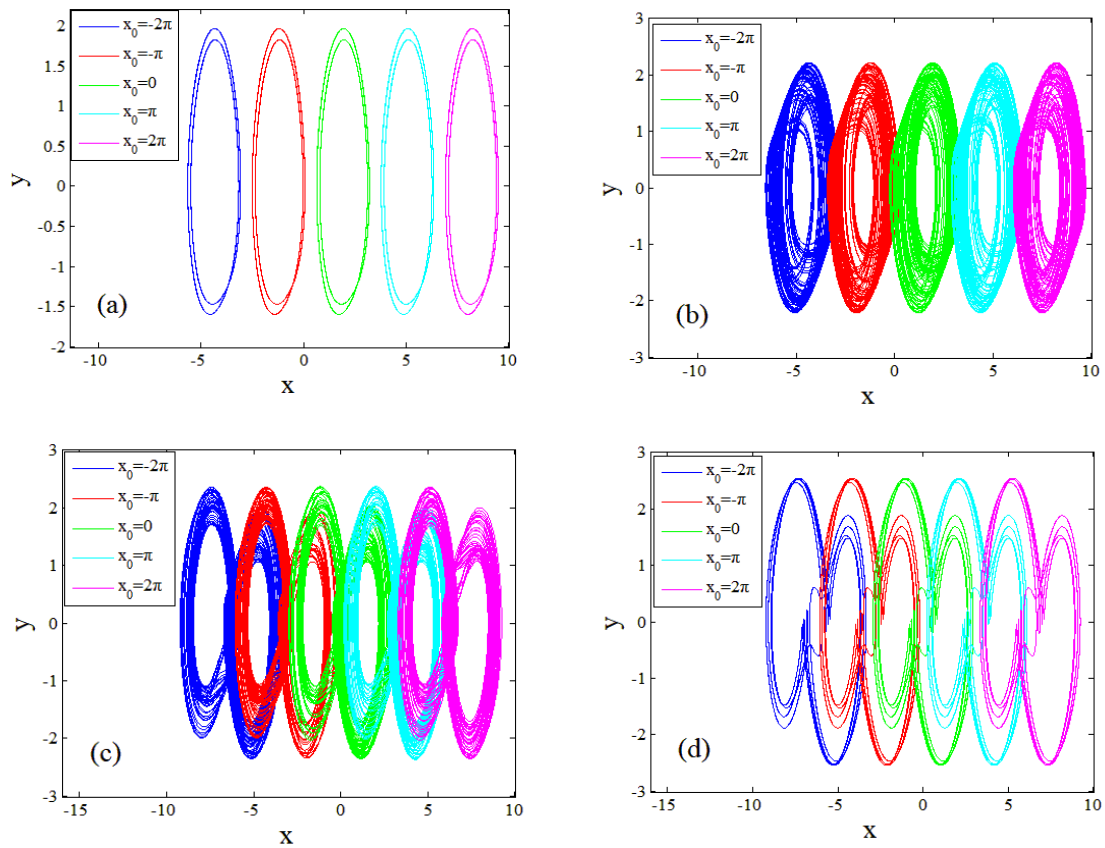


Figure 6. Cont.

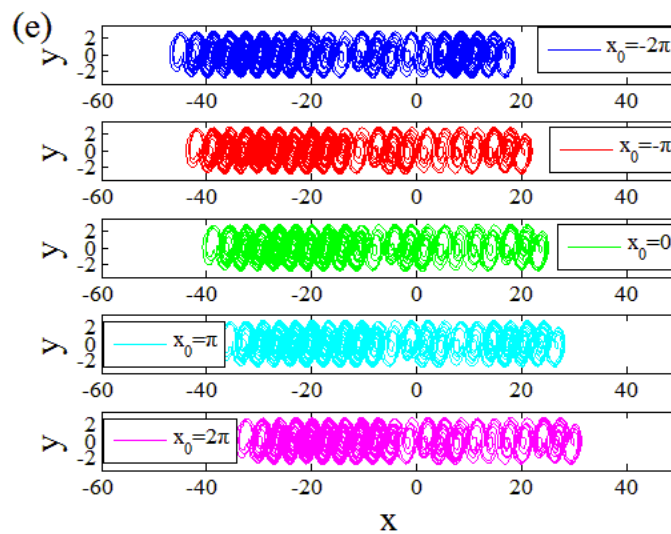


Figure 6. Multi-stable dynamics of the (a) single scroll period-2 when $c = 0.95$; (b) single-scroll chaos when $c = 1.1$; (c) double-scroll chaos when $c = 1.25$; (d) double-scroll period-4 when $c = 1.58$; (e) multi-scroll chaos when $c = 1.8$.

In addition, it can be seen from Figure 5 that within one cycle interval of the initial value x_0 , the system presents variant attractors with different amplitudes, different offsets, or different shapes, as explained by the phase diagrams in Figure 7. In the figure, the parameters and initial conditions were $a = 1.5, b = 0.6, c = 1.0, d = 2, y_0 = 0.01, z_0 = 0.01$.

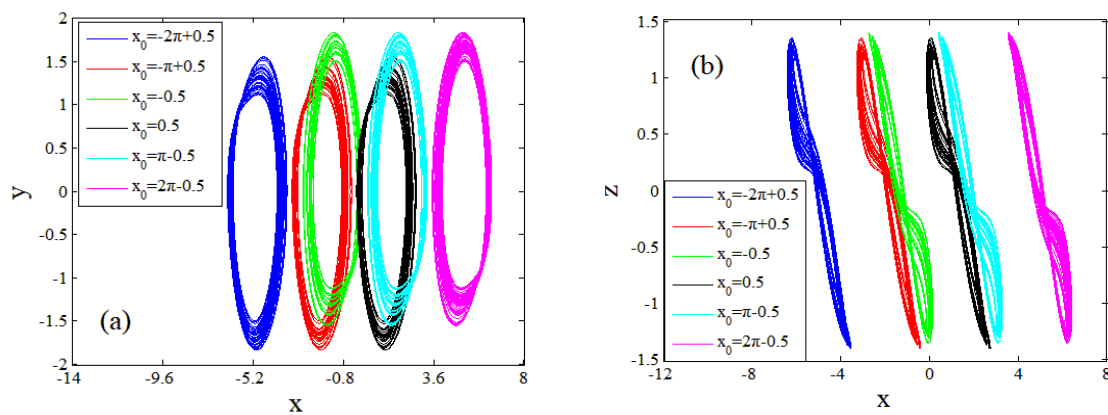


Figure 7. Attractors with different amplitudes, offsets, or shapes in (a) x - y plane; (b) x - z plane.

Meanwhile, the initial values y_0 and z_0 could realize the offset control of variables x and y , and the amplitude control of variable z , but the controlling processes were not periodic, as shown by the bifurcation diagram of the initial values y_0 and z_0 and the corresponding Lyapunov exponent spectra in Figures 8 and 9.

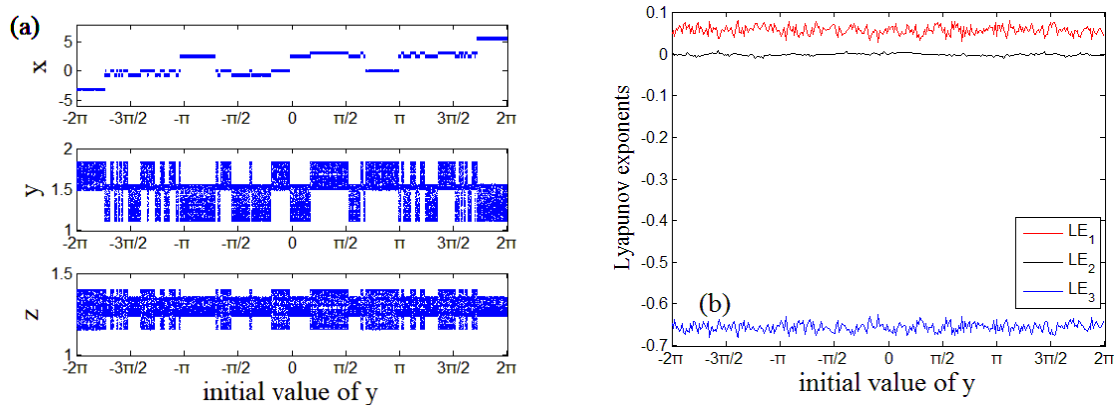


Figure 8. (a) Bifurcation diagram and (b) Lyapunov exponent spectra versus initial value y_0 , when $a = 1.5$, $b = 0.6$, $c = 1.0$, $d = 2$, $x_0 = 0.1$, $z_0 = 0.1$.

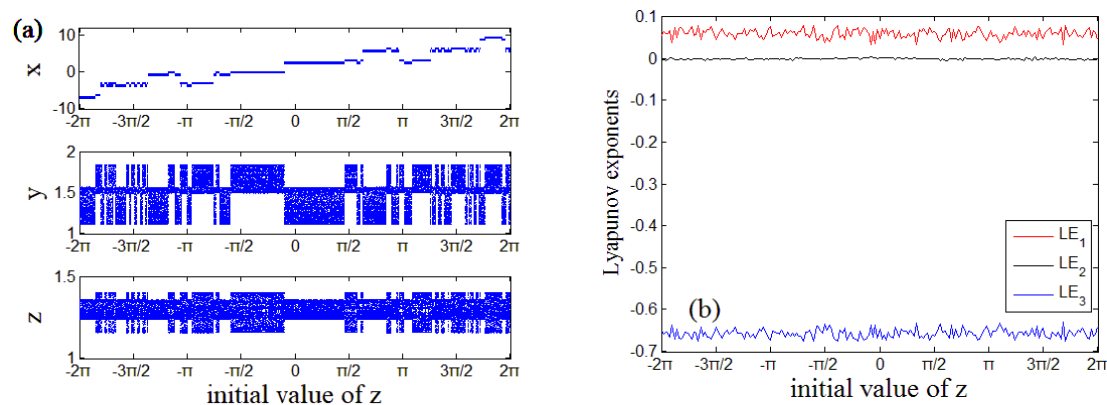


Figure 9. (a) Bifurcation diagram and (b) Lyapunov exponent spectra versus initial value z_0 , when $a = 1.5$, $b = 0.6$, $c = 1.0$, $d = 2$, $x_0 = 0.1$, $y_0 = 0.01$.

The attractor basin of the dynamical system is a set of initial states that result in a long-time motion close to the desired attractor. In other words, the qualitative behavior of the long-term motion of a given system may be fundamentally different according to the domain of the attraction to which the initial condition belongs. The attractors of different basins can be fixed points, limiting the cycles of various periods, quasi-periodic, chaotic, or hyperchaotic orbits. Therefore, the attractor basin can provide more detailed information about the multi-steady state of the dynamical system. Figure 10 shows the attractor basin of the system in the x_0 - z_0 plane with $y_0 = 0.02$ and the attractor basin of the system in the y_0 - z_0 plane with $x_0 = 0.02$, when the parameter condition $a = 1.5$, $b = 0.6$, $c = 1.0$, $d = 2$ and the sampling number 120×120 in the plane of the initial condition are considered. It can be seen from Figure 9 that under the considered parameters and initial conditions, the attractor basin has six different color domains, indicating that the system has six different types of attractors (respectively, named as T1, T2, T3, T4, T5, and T6). Figure 11a,b display the phase diagrams based on the initial conditions corresponding to different color regions in Figure 10a,b. It can be seen that under the initial conditions corresponding to different colors, different types of attractors of the Jerk system can be obtained, which further confirms the multi-stable characteristics of the system. In addition, the system has a relatively wide chaotic region of the system parameters, as can be seen in Figures 1 and 2. Therefore, the parametric error will have a small impact on the structure of the attractor basin.

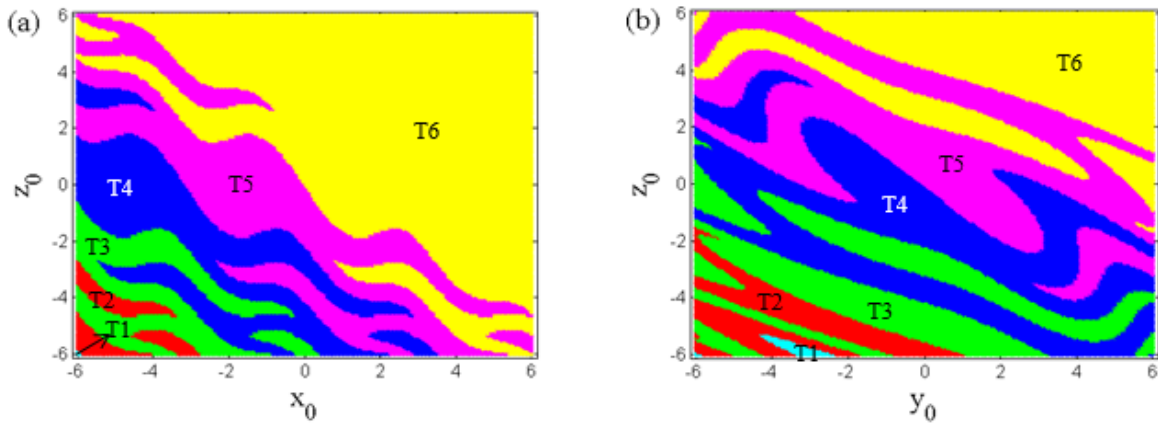


Figure 10. Attractor basin in the (a) x_0 - z_0 plane when $y_0 = 0.02$ and (b) y_0 - z_0 plane when $x_0 = 0.02$.

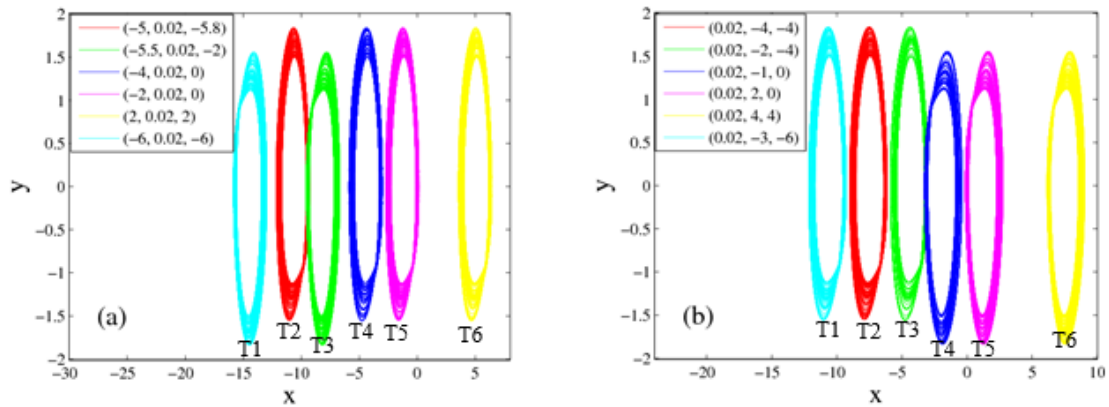


Figure 11. Coexistence attractor with (a) different x_0 and z_0 ; (b) different y_0 and z_0 .

5. Circuit Verification of Jerk System

The hardware implementation realized by the electric element is necessary for the dynamical model in a practical engineering application. Thus, circuit verification for the Jerk system was designed and manufactured in this section. The circuit schematic diagram of system (1) is displayed in Figure 12.

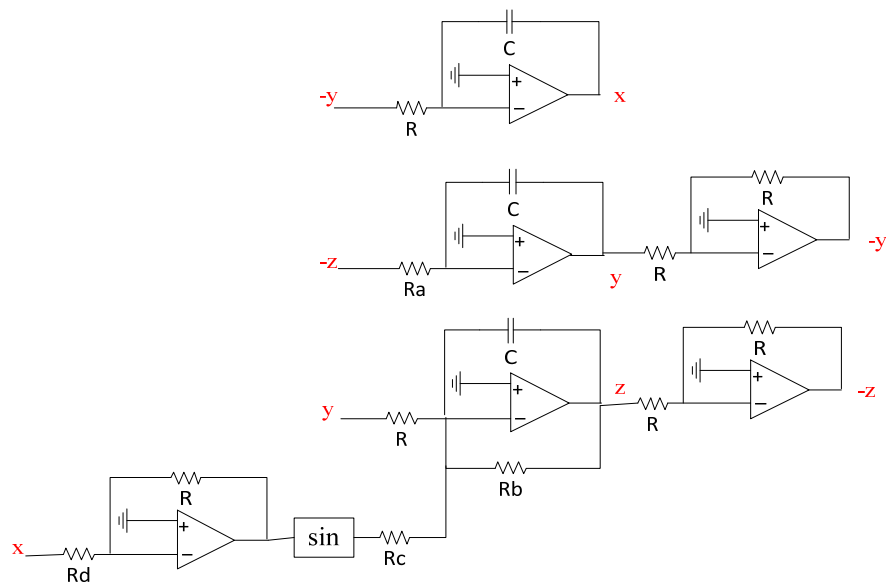


Figure 12. Circuit schematic diagram of the system (1).

The sinusoidal function can be realized by the Taylor expansion [40], as below

$$\sin(x) = x - \frac{x^3}{3!} + \frac{x^5}{5!} - \frac{x^7}{7!} + \dots \tag{3}$$

Then, the sinusoidal function is realized by the multiplier and the operational amplifier, as shown in Figure 13.

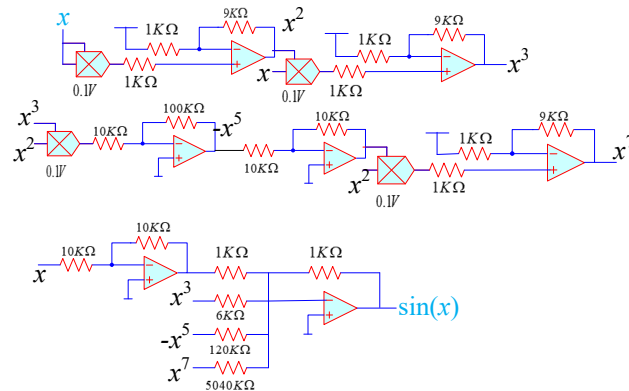


Figure 13. Realization circuit of the sinusoidal function.

Thus, the corresponding circuit state equations are established as

$$\begin{aligned} \frac{dx}{dt} &= \frac{1}{RC}y \\ \frac{dy}{dt} &= \frac{1}{R_a C}z \\ \frac{dz}{dt} &= -\frac{1}{RC}y - \frac{1}{R_b C}z + \frac{1}{R_c C} \sin\left(\frac{R}{R_d}x\right) \end{aligned} \tag{4}$$

When considering $a = 2, b = 0.6, d = 2, C = 100 \text{ nF}$, the resistance values are calculated as $R = 10 \text{ k}\Omega, R_a = R/a = 5 \text{ k}\Omega, R_b = R/b = 16.7 \text{ k}\Omega, R_d = R/d = 5 \text{ k}\Omega$.

As an example of the explanation, parameter c is adjusted to the experiment. When the value of c is set to be 0.8, 1.1, 1.25, and 1.8, the synchronous adjustment resistance R_c is, respectively, calculated as 12.5 kΩ, 9.1 kΩ, 8 kΩ, and 5.6 kΩ. The captured phase diagrams by the experiment are displayed in Figure 14. The experimental results coincide well with the numerical simulations in Figure 3, which proves the physical realizability of the proposed system.

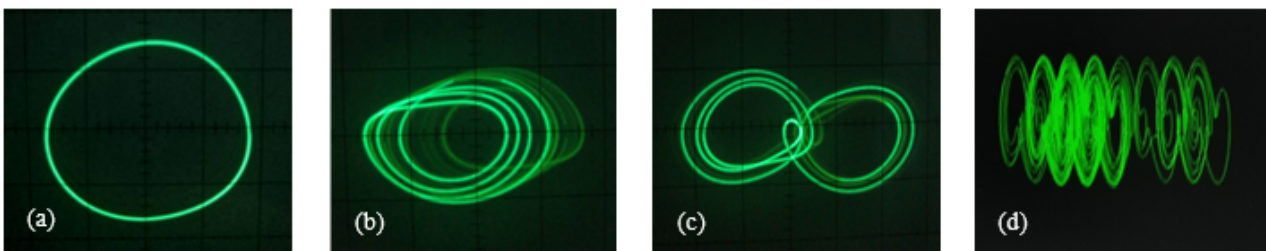


Figure 14. Experimental observation when (a) $R_c = 12.5 \text{ k}\Omega$; (b) $R_c = 9.1 \text{ k}\Omega$; (c) $R_c = 8 \text{ k}\Omega$; (d) $R_c = 5.6 \text{ k}\Omega$.

6. Conclusions

A multi-scroll–multi-stable nonlinear system can generate complex random sequences, which have important application value in data security protection and other fields. However, current studies on multi-scroll–multi-steady behavior have been conducted separately, rather than simultaneously. Therefore, it is of great practical significance to study and effectively control the multi-scroll–multi-steady behavior of a nonlinear system simultaneously. In this paper, a three-dimensional Jerk system with a sinusoidal nonlinear term

was considered. It was found that the system has infinite line equilibrium points. Thus, based on the interior relation of the equilibrium point and scroll, the sinusoid nonlinearity-based Jerk system can generate multi-scroll attractors. Moreover, the Jerk system can realize the self-reproduction of these dynamical behaviors by controlling the initial value. Therefore, we can realize the effective control of structural diversity and state diversity of the Jerk system at the same time by expanding the equilibrium point, which will greatly increase the complexity of the system and its application in random number generation and data security.

Author Contributions: Conception: F.L. and J.Z.; experimental conception and design: F.L.; experiment implementation: F.L.; software simulation: F.L. and J.Z.; data analysis: F.L. and J.Z.; writing: F.L. All authors have read and agreed to the published version of the manuscript.

Funding: This work was supported in part by the Enterprise scientific research project “Research on monitoring system of wind-solar storage-charge microgrid” (no. S2026118).

Data Availability Statement: The data used to support the findings of this study are included within the article.

Conflicts of Interest: The authors declare no conflict of interest.

References

- Gómez-Guzmán, L.; Cruz-Hernandez, C.; Gutierrez, R.M.L.; Guerrero, E.E.G. Synchronization of Chua’s Circuits with Multi-Scroll Attractors: Application to Communication. *Commun. Nonlinear Sci. Numer. Simul.* **2009**, *14*, 2765–2775. [\[CrossRef\]](#)
- Zhou, Y.; Li, C.; Li, W.; Li, H.; Feng, W.; Qian, K. Image encryption algorithm with circle index table scrambling and partition diffusion. *Nonlinear Dyn.* **2021**, *103*, 2043–2061. [\[CrossRef\]](#)
- Yildirim, M. Optical color image encryption scheme with a novel DNA encoding algorithm based on a chaotic circuit. *Chaos Solitons Fractals* **2022**, *155*, 111631. [\[CrossRef\]](#)
- Li, C.L.; Zhou, Y.; Li, H.M.; Feng, W.; Du, J. Image encryption scheme with bit-level scrambling and multiplication diffusion. *Multimed. Tools Appl.* **2021**, *80*, 18479–18501. [\[CrossRef\]](#)
- Yang, H.; Xu, X.; Jiang, G.; Luo, R. A Novel Multi-User Carrier Index Differential Chaos Shift Keying Modulation Scheme. *J. Circuits Syst. Comput.* **2022**, *31*, 2350009. [\[CrossRef\]](#)
- Ding, P.; Feng, X. Generation of Multi-Scroll Chaotic Attractors from a Jerk Circuit with a Special Form of a Sine Function. *Electronics* **2020**, *9*, 842. [\[CrossRef\]](#)
- Tlelo-Cuautle, E.; Rangel-Magdaleno, J.J.; Pano-Azucena, A.D.; Obeso-Rodelo, P.J.; Nuñez-Perez, J.C. FPGA realization of multi-scroll chaotic oscillators. *Commun. Nonlinear Sci. Numer. Simul.* **2015**, *27*, 66–80. [\[CrossRef\]](#)
- Mathale, D.; Goufo, E.; Khumalo, M. Coexistence of multi-scroll chaotic attractors for a three-dimensional quadratic autonomous fractional system with non-local and non-singular kernel. *Alex. Eng. J.* **2021**, *60*, 3521–3538. [\[CrossRef\]](#)
- Li, C.L.; Yu, S.; Luo, X. A ring-scroll Chua system. *Int. J. Bifurc. Chaos* **2023**, *23*, 1350170. [\[CrossRef\]](#)
- Altun, K. Multi-Scroll Attractors with Hyperchaotic Behavior Using Fractional-Order Systems. *J. Circuits Syst. Comput.* **2022**, *31*, 2250085. [\[CrossRef\]](#)
- Li, C.L.; Li, Z.Y.; Feng, W.; Tong, Y.N.; Wei, D.Q. Dynamical behavior and image encryption application of a memristor-based circuit system. *AEU-Int. J. Electron. Commun.* **2019**, *110*, 152861. [\[CrossRef\]](#)
- Zambrano-Serrano, E.; Munoz-Pacheco, J.M.; Serrano, F.E.; Sánchez-Gaspariano, L.A.; Volos, C. Experimental verification of the multi-scroll chaotic attractors synchronization in PWL arbitrary-order systems using direct coupling and passivity-based control. *Integr. VLSI J.* **2021**, *81*, 56–70. [\[CrossRef\]](#)
- Peng, Y.; He, S.; Sun, K. Parameter identification for discrete memristive chaotic map using adaptive differential evolution algorithm. *Nonlinear Dyn.* **2022**, *7*, 1263–1275. [\[CrossRef\]](#)
- Li, C.; Yang, Y.; Yang, X.; Zi, X.; Xiao, F. A tristable locally active memristor and its application in Hopfield neural network. *Nonlinear Dyn.* **2022**, *108*, 1697–1717. [\[CrossRef\]](#)
- Ding, P.; Feng, X.; Lin, F. Generation of 3-D Grid Multi-Scroll Chaotic Attractors Based on Sign Function and Sine Function. *Electronics* **2020**, *9*, 2145. [\[CrossRef\]](#)
- Li, H.; Lu, Y.; Li, C. Dynamics in stimulation-based tabu learning neuron model. *Int. J. Electron. Commun.* **2021**, *142*, 153983. [\[CrossRef\]](#)
- Li, C.; Li, H.; Xie, W.; Du, J. A S-type bistable locally active memristor model and its analog implementation in an oscillator circuit. *Nonlinear Dyn.* **2021**, *106*, 1041–1058. [\[CrossRef\]](#)
- Suykens, J.; Vandewalle, J. Generation of n-double scrolls (n=1,2,3,4,...). *IEEE Trans. Circuits Syst.-I* **1993**, *40*, 861–867. [\[CrossRef\]](#)
- Yu, S.; Tang, W.K.S.; Lu, J. Generating 2n-wing attractors from Lorenz-like systems. *Int. J. Circuit Theory Appl.* **2010**, *38*, 243–258. [\[CrossRef\]](#)

20. Yu, S.; Tang, W.K.S. Generation of $n \times m$ -scroll attractors in a two-port RCL network with hysteresis circuits. *Chaos Soliton Fract.* **2009**, *39*, 821–830. [[CrossRef](#)]
21. Hu, X.; Liu, C.; Liu, L.; Ni, J.; Li, S. Multi-scroll hidden attractors in improved Sprott A system. *Nonlinear Dyn.* **2016**, *86*, 1725–1734. [[CrossRef](#)]
22. Wang, F.; Liu, C. Generation of multi-scroll chaotic attractors via the saw-tooth function. *Int. J. Mod. Phys. B* **2008**, *22*, 2399–2405. [[CrossRef](#)]
23. Lü, J.; Han, F.; Yu, X.; Chen, G. Generating 3-D multi-scroll chaotic attractors: A hysteresis series switching method. *Automatica* **2004**, *40*, 1677–1687. [[CrossRef](#)]
24. Li, C.; Qian, K.; He, S.; Li, H.; Feng, W. Dynamics and optimization control of a robust chaotic map. *IEEE Access* **2019**, *7*, 160072–160081. [[CrossRef](#)]
25. Ma, C.; Mou, J.; Cao, Y.; Liu, T.; Wang, J. Multistability analysis of a conformable fractional-order chaotic system. *Phys. Scr.* **2020**, *7*, 075204. [[CrossRef](#)]
26. Chen, L.; Peng, H.; Wang, D. Studies on the construction method of a family of multi-scroll chaotic systems. *Acta Phys. Sin.* **2008**, *57*, 3337–3341. [[CrossRef](#)]
27. Yu, S.; Lü, J.; Yu, X.; Chen, G. Design and implementation of grid multiwing hyperchaotic Lorenz system family via switching control and constructing super-heteroclinic loops. *IEEE Trans Circuits Syst-I* **2012**, *59*, 1015–1028. [[CrossRef](#)]
28. Li, C.; Hai, W. Constructing multiwing attractors from a robust chaotic system with non-hyperbolic equilibrium points. *Automatika* **2018**, *59*, 184–193. [[CrossRef](#)]
29. Ai, X.; Sun, K.; He, S.; Wang, H. Design of Grid Multiscroll Chaotic Attractors via Transformations. *Int. J. Bifurc. Chaos* **2015**, *25*, 1530027. [[CrossRef](#)]
30. Wang, Z.; Ma, J.; Cang, S.; Wang, Z.; Chen, Z. Simplified hyper-chaotic systems generating multi-wing non-equilibrium attractors. *Optik* **2016**, *127*, 2424–2431. [[CrossRef](#)]
31. Ramadoss, J.; Kengne, J.; Koinfo, J.B.; Rajagopal, K. Multiple Hopf bifurcations, period-doubling reversals and coexisting attractors for a novel chaotic jerk system with Tchebychev polynomials. *Phys. A* **2022**, *587*, 126501. [[CrossRef](#)]
32. Ma, J.; Wu, X.; Chu, R.; Zhang, L. Selection of multi-scroll attractors in Jerk circuits and their verification using Pspice. *Nonlinear Dyn.* **2014**, *76*, 1951–1962. [[CrossRef](#)]
33. Guo, M.; Zhu, Y.; Liu, R.; Zhao, K.; Dou, G. An associative memory circuit based on physical memristors. *Neurocomputing* **2022**, *472*, 12–23. [[CrossRef](#)]
34. Li, C.; Chen, Z.; Yang, X.; He, S.; Du, J. Self-reproducing dynamics in a two-dimensional discrete map. *Eur. Phys. J. Spec. Top.* **2021**, *230*, 1959–1970. [[CrossRef](#)]
35. Wang, X.Y.; Dong, C.T.; Zhou, P.F.; Nandi, S.K.; Nath, S.K.; Elliman, R.G.; Iu, H.H.; Kang, S.M.; Eshraghian, J.K. Low-Variance Memristor-Based Multi-Level Ternary Combinational Logic. *IEEE Trans. Circuits Syst. I* **2022**, *69*, 2423–2434. [[CrossRef](#)]
36. Njitacke, Z.T.; Fotsin, H.B.; Negou, A.N.; Tchiotso, D. Coexistence of Multiple Attractors and Crisis Route to Chaos in a Novel Chaotic Jerk Circuit. *Int. J. Bifurc. Chaos* **2016**, *26*, 1650081.
37. Li, H.D.; Li, C.L.; Du, J.R. Discretized locally active memristor and application in logarithmic map. *Nonlinear Dyn.* **2022**, *16*, 736642. [[CrossRef](#)]
38. Marszalek, W.; Sadecki, J. Complex two-parameter bifurcation diagrams of a simple oscillating circuit. *IEEE Trans. Circuits Syst. II* **2018**, *66*, 687–691. [[CrossRef](#)]
39. Li, C.; Li, H.; Li, W.; Tong, Y.; Zhang, J.; Wei, D.; Li, F. Implementation and stability of a chaotic system with coexistence of hyperbolic and non-hyperbolic equilibria. *Int. J. Electron. Commun.* **2018**, *84*, 199–205. [[CrossRef](#)]
40. Wang, M.; Li, J.; Zhang, X.; Iu, H.H.-C.; Fernando, T.; Li, Z.; Zeng, Y. A novel non-autonomous chaotic system with infinite 2-D lattice of attractors and bursting oscillations. *IEEE Trans. Circuits Syst. II* **2020**, *68*, 1023–1027. [[CrossRef](#)]

Disclaimer/Publisher’s Note: The statements, opinions and data contained in all publications are solely those of the individual author(s) and contributor(s) and not of MDPI and/or the editor(s). MDPI and/or the editor(s) disclaim responsibility for any injury to people or property resulting from any ideas, methods, instructions or products referred to in the content.